[Chem. Pharm. Bull. 27(6)1412—1421(1979)]

UDC 539.22.08 : 547.922.03.08

The Effect of Alkanes as Solutes on the Transition Temperatures of Liquid Crystal Substances: Cholesteryl Myristate and Cholesteryl Palmitate

Isamu Miyata and Hiroshi Kishimoto

Faculty of Pharmaceutical Sciences, Nagoya City University[1]

(Received December 13, 1978)

Transition temperatures between coexisting (solid-smectic, solid-cholesteric, smectic-cholesteric and cholesteric-isotropic liquid phases) of cholesteryl myristate (ChM) and cholesteryl palmitate (ChP) were studied by differential scanning calorimetry (DSC) as well as polarized light microscopy, in the presence and absence of *n*-heptane, *n*-octane and *n*-nonane as solutes.

The polymorphism of ChM and ChP was maintained in spite of the addition of *ca.* 0.06 molar ratio of alkanes, although the distinction between coexisting phases decreased in enthalpy and entropy terms, resulting in the disappearance of liquid crystal phases (smectic and cholesteric phases).

The addition of alkanes markedly depressed the transition temperatures; this could be described quantitatively by thermodynamic analysis, taking into consideration the partition of alkanes between coexisting phases. The partition coefficients and the molar transition excess enthalpies of alkanes on mixing with ChM and ChP were calculated by simulation. The partition coefficients obtained from the DSC study agreed reasonably well with those previously determined by gas–liquid chromatography.

Keywords——liquid crystal; cholesteryl myristate; cholesteryl palmitate; smectic phase; cholesteric phase; DSC; polymorphism; phase transition temperature; partition coefficient; transition excess enthalpy

Introduction

The structures of liquid crystal substances[2] often change remarkably with changes of electrical or thermal environment or upon the addition of a small amount of soluble component. These responses often result in specific optical characteristics and have led to wide applications of liquid crystal substances, including clinical uses.[3] The behavior of liquid crystal structures is also of biological interest, since they exist in many biological tissues, especially in membrane structures,[4] playing important roles in the transfer of material, energy or information. Thus, drugs may interact with or pass through biological liquid crystal structures, possibly affecting the transfer properties of membranes towards essential chemicals. We have therefore studied the interaction between liquid crystal substances and trace amounts of soluble compounds (solutes) by gas–liquid chromatography.[5,6]

In the present work, we investigated the structural effects of mixing various amounts of solutes with liquid crystal substances by measurements of the phase transition temperature and enthalpy as well as by polarized light microscopy of liquid crystals.

1) Location: *Tanabe-dori, Mizuho-ku, Nagoya, 467, Japan.*
2) T. Tachibana, K. Kobayashi, S. Kusabayashi, H. Suzuki, K. Honda, and M. Sukigara, "Ekisho," Kyoritsu-Shuppan, Tokyo, 1972.
3) S. Iwayanagi and Y. Sugiura, *Seibutsubutsuri*, **15**, 164 (1972).
4) O.S. Selawry, H.S. Selawry, and J.F. Holland, *Mol. Cryst.*, **1**, 495 (1966).
5) I. Miyata and H. Kishimoto, *Yakugaku Zasshi*, **98**, 689 (1978).
6) I. Miyata and H. Kishimoto, *Yakugaku Zasshi*, **98**, 1629 (1978).

Experimental

Materials and Apparatus

Liquid Crystal Substances——Cholesteryl myristate (ChM: Tokyo Kasei Kōgyo Co., Ltd.) and cholesteryl palmitate (ChP: Tokyo Kasei Kōgyo Co., Ltd.) were used after several recrystallizations from ethanol.

Solute——Heptane, octane and nonane were from Tokyo Kasei Kōgyo Co., Ltd. (Standard Kit, Special Grade).

Differential Scanning Calorimeter (DSC)——A TG-DSC unit was used (Hyojungata, Rigakudenki Co., Ltd.).

Microphotographic Apparatus——A microscope (Model POS, Olympus Kōgaku Kōgyo Co., Ltd.) and camera (PFM F2, Nihon Kōgaku Kōgyo Co., Ltd.), were used.

Procedures

Polarized light microphotographs were taken of pure ChM and ChP, which were heated at a rate of *ca.* 2 K min^{-1}.

For DSC, a pure liquid crystal or mixtures with various solutes were weighed in a glass ampoule (2 ml), melted at *ca.* 363 K after sealing the ampoule, and cooled to room temperature with vigorous shaking, giving solidified samples. Immediately after removal from the ampoule, *ca.* 7—10 mg of sample was sealed into an aluminum holder. The sealed sample was heated at a controlled rate of 2.5 K min^{-1} (heating curve) and allowed to cool to 310 K (cooling curve) in the DSC apparatus. The sensitivity of the calorimeter was ± 16.7 mJ s^{-1}.

Results and Discussion

Definitions of Characteristic Points in the DSC Curve

The DSC output, *i.e.*, rate of endothermic heat flow, $\dot{q}$, *versus* time, gives a curve of the type shown in Fig. 1, which has reasonably gentle slopes on both sides of the peak, p. We used the initial and final points, i and f, as measures of the width of the peak. Both points were obtained as the intersections of extrapolations of the linear parts of the plots with the

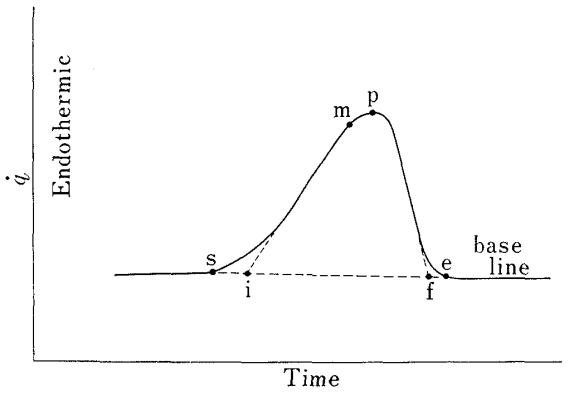

Fig. 1. Typical DSC Curve at a Phase Transition

See the text for the meaning of each symbol.

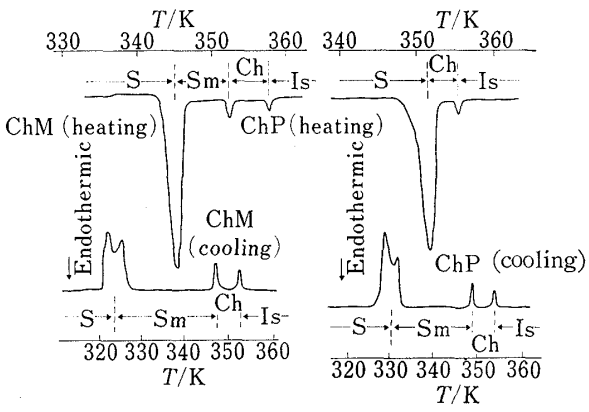

Fig. 2. DSC Curves of Pure ChM and ChP

controlled heating: 2.5 K min^{-1},
natural cooling: 90 min from 370 K to 310 K.
S: solid, Sm: smectic phase, Ch: cholesteric phase,
Is: isotropic liquid.

1) cholesteryl myristate (ChM)

solid ⇄ smectic phase ⇄ cholesteric phase ⇄ isotropic liquid

2) cholesteryl palmitate (ChP)

solid ← smectic phase ⇄ cholesteric phase ⇄ isotropic liquid

Chart 1. Transition Paths of ChM and ChP

⟶: heating, ⟵: cooling.

base lines. The integration of the DSC curve from the starting point, s, to the end point, e, gives the enthalpy of transition, ΔH. We denote the point corresponding to the half-value of integrated heat by m; that is, the reaction is half completed at this time.

Pure ChM and ChP

DSC curves of pure ChM and ChP are shown in Fig. 2, with temperature on the abscissa. The scheme of phase transitions of ChM and ChP is presented in Chart 1. It was found that the transition path of ChM was reversible with respect to temperature, although slight lags of transition were noted. However, the path of ChP was irreversible, that is, the smectic phase was found on cooling, though it was absent on heating. On cooling of ChM and ChP, splitting of the peak at the smectic-solid phase transition was always observed, implying that this transition is complex. This was not studied further in this work. The identification of each phase was done by comparison of our DSC and polarized light microscopic (visual or photographic) observations with the literature descriptions.[7]

Mixed Systems

DSC curves of ChM-nonane systems having various compositions are shown in Fig. 3. With increasing mole fraction of solute (x_2), the endothermic peaks became broad, which was indicated in Fig. 4 by the increasing distance between the two temperatures corresponding

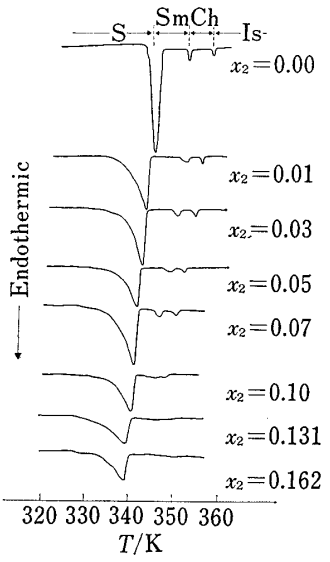

Fig. 3. DSC Curves of ChM-Nonane Mixed Systems

controlled heating rate: 2.5 K min^{-1}
S: solid, Sm: smectic phase, Ch: cholesteric phase, Is: isotropic phase.

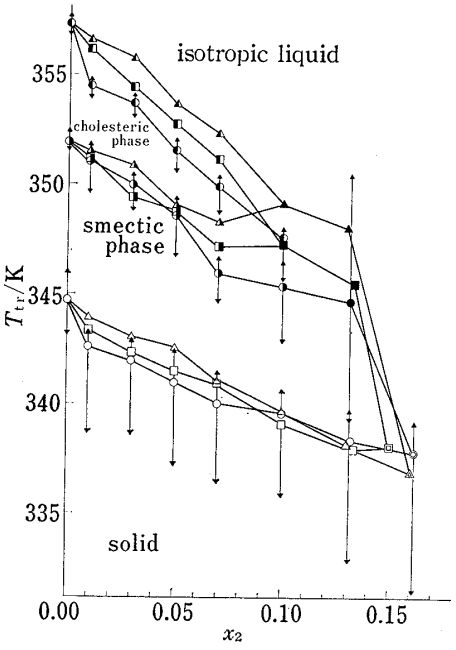

Fig. 4. Phase Diagrams of ChM-Alkane Systems

Empty symbols (△,□,○), right half-filled symbols (◭,◨,◑), left half-filled symbols (◮,◧,◐), solid symbols (▲,■,●), and double symbols (◬,⧈,◎) denote the characteristic temperatures, T_{tr}, corresponding to point p in Fig. 1 at the solid-smectic, smectic-cholesteric, cholesteric-isotropic, smectic-isotropic and solid-isotropic transitions, respectively; triangular, square and circular symbols correspond to *n*-heptane, *n*-octane and *n*-nonane, respectively.

The two arrow-heads projecting from each symbol for the ChM-nonane system denote the two temperatures corresponding to points i and f in Fig. 1.

7) G.H. Brown, G.J. Dienes, and M.M. Labes, "Liquid Crystal," Gordon and Breach, Sci. Publ., New York, 1966, pp. 341—362.

to points i and f on the DSC curve at each transition. Near x_2=0.13, the distinction between isotropic or smectic phase and cholesteric phase could no longer be observed; the cholesteric phase disappeared. At higher contents of solute, the distinction between liquid crystal phases and isotropic liquid phase disappeared. The transition temperature, T_{tr}, corresponding to the point p in Fig. 1, gradually fell as x_2 increased. The slopes of curves for T_{tr} *vs.* x_2 of solid-smectic, smectic-cholesteric, and cholesteric-isotropic phase transitions were almost the same up to x_2= *ca.* 0.07. In the presence of heptane or octane in ChM, the similar behavior was found in the DSC curves, which are also shown in terms of T_{tr} *vs.* x_2 relations in Fig. 4. It was found that, the slope for each transition became steeper as the alkane content increased. Heptane or octane made the cholesteric phase disappear at lower x_2, *i.e.*, near x_2=0.10, than nonane.

In the case of ChP-alkane systems, two kinds of T_{tr} *vs.* x_2 plots were obtained: (i) on simple heating, there were transitions of solid-cholesteric and cholesteric-isotropic phases as shown in Fig. 5 and (ii) on heating the smectic phase which was produced by cooling of the cholesteric phase, there were transitions of smectic-cholesteric and cholesteric-isotropic phases as shown in Fig. 6. In the latter case, T_{tr} of the smectic-solid transition on cooling was difficult to determine owing to the nature of the transition: supercooling occurred with poor reproducibility and flatness of the DSC curve. On simple heating (Fig. 5) of ChP-alkane systems, the temperature range of the cholesteric phase was a little narrower than in ChM-alkane systems, probably due to the difference between the extents of the cholesteric regions of pure ChM and ChP. Since ChP has no smectic phase in this procedure, its liquid crystal phase region was significantly narrower than that of ChM, which has cholesteric and smectic liquid crystal phases. The effects of amount and chain length of alkane on ChP transitions were similar to those with ChM. In the second procedure (Fig. 6), the transitions of smectic-cholesteric and cholesteric-isotropic phases of ChP were similar to those of ChM both in the presence and absence of alkanes. With the addition of alkanes, the cholesteric phase of ChP disappeared sooner than that of ChM. Dividing the enthalpy of transition, ΔH, which was obtained by integration of the DSC curve, by the amount of liquid crystal (component 1), we can approximately obtain the partial molar transition enthalpy, ΔH_1, of the liquid crystal. The relationship between ΔH_1 of ChM or ChP and x_2 are shown in Figs. 7 and 8.

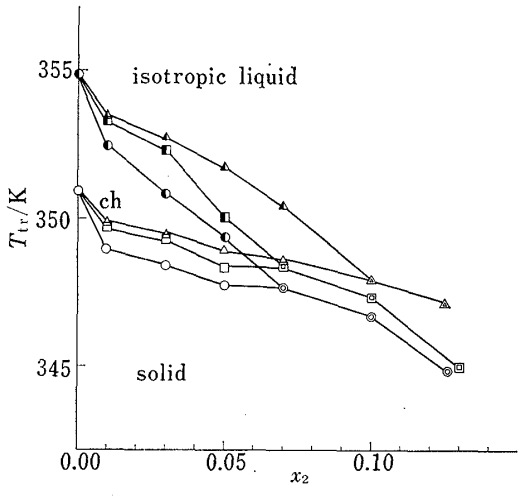

Fig. 5. Phase Diagrams of ChP-Alkane Systems on Simple Heating

Each symbol is the same as in Fig. 4, except that empty symbols (△,□,○) denote T_{tr} at the solid-cholesteric transition.
ch: cholesteric phase.

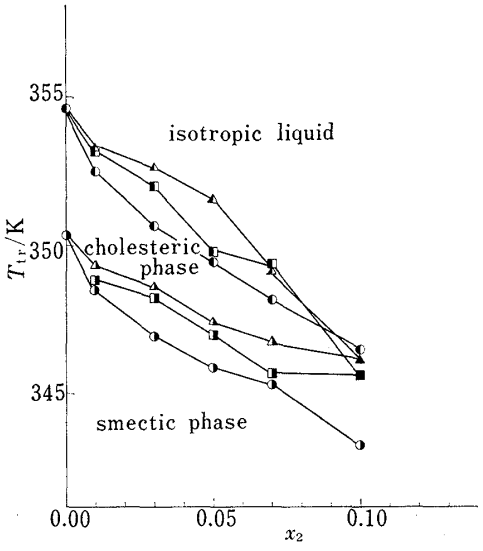

Fig. 6. Phase Diagrams of ChP-Alkane Systems on Heating of the Monotropic Smectic Phase

Symbols are the same as in Fig. 4.

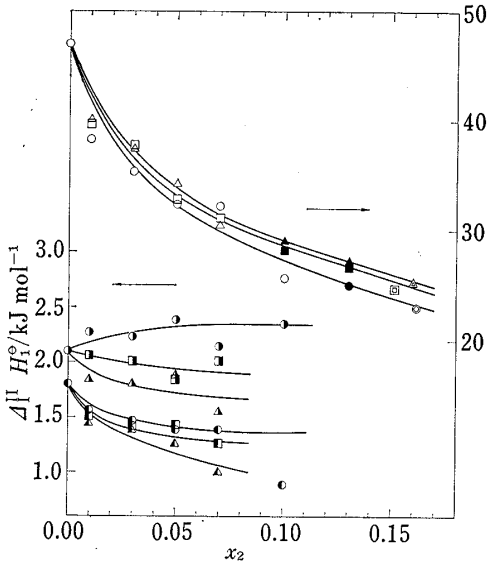

Fig. 7. Relation between the Transition Molar Enthalpy of ChM, $\Delta_I^{II} H_1^\ominus$ and the Molar Fraction of *n*-Alkane, x_2

The symbols are analogous to the symbols used in Fig. 4, where they correspond to T_{tr}. However, in this figure the symbols correspond to $\Delta_I^{II} H_1^\ominus$.

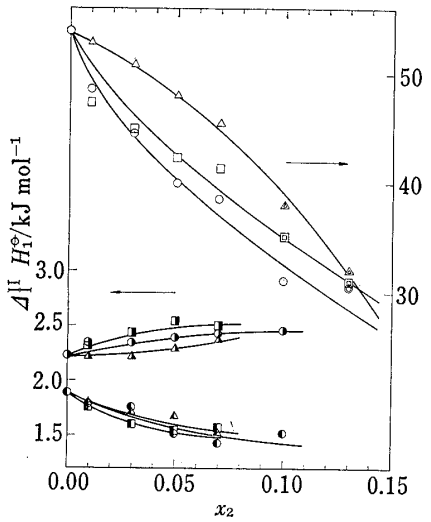

Fig. 8. Relation between the Transition Molar Enthalpy of ChP, $\Delta_I^{II} H_1^\ominus$, and the Molar Fraction of *n*-Alkane, x_2

Symbols are the same as in Fig. 7.

The small value of ΔH_1 of the cholesteric-isotropic transition indicates similarity in energy between the cholesteric and isotropic liquid phases. The introduction of solute into the liquid crystal phase increase this tendency, resulting finally in the disappearance of any distinction between the two phases. With respect to the solid-smectic transition, the directly measured ΔH_1 of the ChM system was compared to the calculated ΔH_1 of the ChP system, *i.e.*, ΔH_1 of the solid-cholesteric transition minus that of the smectic-cholesteric transition. The introduction of solute also appears to reduce the distinction between solid and smectic phases, although the distinction itself was still large. However, the distinction, although small, between the cholesteric and smectic phases was not affected by the presence of solute. As regards the effect of solute chain length on ΔH_1, higher alkanes seem to decrease ΔH_1 in the solid-smectic transition and increase it in the smectic-cholesteric and cholesteric-isotropic transitions, although scattering of data makes this conclusion tentative, especially in the case of the last transition.

The molar transition entropy of a liquid crystal, ΔS_1, can be obtained as ΔH_1 of each transition divided by T'_{tr}, which corresponds to the point m in Fig. 1. The values of T'_{tr} corresponding to various values of x_2 are plotted in Figs. 11 and 12. The selection of T'_{tr} rather than T_{tr} was based on the fact that at T'_{tr}, but not at T_{tr}, the heat absorbed by the system at transition reached half of the total. A tendency similar to that seen for ΔH_1 can be found for ΔS_1, since T'_{tr} is not greatly different among various transitions of the same liquid crystal substance.

Thermodynamic Analysis of T_{tr} *vs.* x_2

We attempted to describe the dependency of the phase transition temperature of a liquid crystal on the amount of solute thermodynamically. As is usually found in the phase transition between condensed phases, the transition of liquid crystal substance on cooling did not occur at a fixed temperature, due to overcooling. The transition on heating always occurred at the same temperature. We designated the phases, stable at lower and higher temperatures as phase I and phase II, respectively. First, we shall assume that the equilibrium between phases I and II, each containing components 1 (liquid crystal substance) and 2

(solute), is established at temperature, T. For component 1, the equilibrium molar fractions of which are x_1^{I} and x_1^{II} in phases I and II, respectively, we have

$$\mu_1^{I,\ominus} + \boldsymbol{R}T \ln \gamma_1^{I} x_1^{I} = \mu_1^{II,\ominus} + \boldsymbol{R}T \ln \gamma_1^{II} x_1^{II} \quad (1)$$

where $\mu_1^{I,\ominus}$ and $\mu_1^{II,\ominus}$ represent the standard chemical potentials and γ_1^{I} and γ_1^{II} the activity coefficients of component 1 in phases I and II, respectively. Then, the standard transition chemical potential of component 1, $\Delta_I^{II}\mu_1^{\ominus}$, can be written as follows.

$$\Delta_I^{II}\mu_1^{\ominus} \equiv \mu_1^{II,\ominus} - \mu_1^{I,\ominus} = -\boldsymbol{R}T[\ln(\gamma_1^{II}/\gamma_1^{I}) + \ln(x_1^{II}/x_1^{I})] \quad (2)$$

Since $\ln x_1 = \ln(1-x_2) \approx -x_2 - (x_2)^2/2$ for small x_2, Eq. (2) can be readily transformed to Eq. (3).

$$\Delta_I^{II}\mu_1^{\ominus}/\boldsymbol{R}T + (\ln \gamma_1^{II} - \ln \gamma_1^{I}) = (x_2^{II} - x_2^{I})\left[1 + \frac{1}{2}(x_2^{II} + x_2^{I})\right] \quad (3)$$

where x_2^{I} and x_2^{II} are the equilibrium molar fractions of component 2 in phases I and II, respectively. Differentiating Eq. (3) by T at constant pressure and using a modification of the Gibbs-Helmholz relation, *i.e.*, $[\partial(\mu/T)/\partial T]_p = -H/\boldsymbol{R}T^2$, we have

$$[-\Delta_I^{II}H_1^{\ominus} - (H_1^{II,E} - H_1^{I,E})]/\boldsymbol{R}T^2 = \mathrm{d}\left[(x_2^{II} + x_2^{I})\left\{1 + \frac{1}{2}(x_2^{II} + x_2^{I})\right\}\right]\Big/\mathrm{d}T \quad (4)$$

where $\Delta_I^{II} H_1^{\ominus}$ represents the standard molar transition enthalpy of component 1 and $H_1^{I,E}$ and $H_1^{II,E}$ the excess molar enthalpies[8] in phases I and II, respectively. The molar transition excess enthalpy, $H_1^{II,E} - H_1^{I,E}$ or $\Delta_I^{II} H_1^{E}$, is dependent on the amount of solute and is zero at $x_2 = 0$. Integrating Eq. (4) from T_{tr}^{0}, which represents the phase transition temperature with $x_2 = 0$, to T_{tr} with finite x_2, we have

$$\frac{\Delta_I^{II}H_1^{\ominus} + \overline{\Delta_I^{II}H_1^{E}}}{\boldsymbol{R}} \cdot \frac{T_{tr}^{0} - T_{tr}}{T_{tr}^{0}T_{tr}} = (x_2^{II} - x_2^{I})\left[1 + \frac{1}{2}(x_2^{II} + x_2^{I})\right] \quad (5)$$

where $\overline{\Delta_I^{II}H_1^{E}}$ denotes the mean molar transition excess enthalpy of component 1 from T_{tr}° to T_{tr}, defined by the following relation.

$$\overline{\Delta_I^{II}H_1^{E}} = \frac{\int_{T_{tr}^{0}}^{T_{tr}} (\Delta_I^{II}H_1^{E}/T^2)\partial T}{(1/T_{tr} - 1/T_{tr}^{0})} \quad (6)$$

Denoting x_2^{I}/x_2^{II}, *i.e.*, the partition coefficient of component 2, by r and $T_{tr}^{0} - T_{tr}$ by ΔT_{tr}, we have

$$\Delta T_{tr} = \frac{\boldsymbol{R}T_{tr}T_{tr}^{0}}{\Delta_I^{II}H_1^{\ominus} + \Delta_I^{II}H_1^{E}} \cdot (1-r)x_2^{II} \cdot \left[1 + \frac{1}{2}(1+r)x_2^{II}\right] \quad (7)$$

When the transition temperature is represented by T'_{tr}, corresponding to the point m in Fig. 1, the following alternative relations approximately hold for small x_2.

$$n_1^{II} \approx n_1^{II} \quad (8)$$

or

$$N^{I} \approx N^{II} \quad (9)$$

where n_1^{I} and n_1^{II} represent the molar amounts of component 1 and N^{I} and N^{II} the total molar amounts of components 1 and 2 in phases I and II, respectively. The substitution of Eq. (8) into Eq. (7) gives a rather complicated expression. Consequently, we shall use Eq. (9) hereafter. The molar fraction of component 2 in the sample, x_2, *i.e.*, $(n_2^{I} + n_2^{II})/(N^{I} + N^{II})$, has the following relation with x_2^{I} and x_2^{II} at T'_{tr}.

$$x_2 \approx \frac{n_2^{I}}{2N^{I}} + \frac{n_2^{II}}{2N^{II}} = \frac{1}{2}(x_2^{I} + x_2^{II}) \quad (10)$$

Alternatively, x_2^{II} can be given by x_2 and r at T'_{tr} as follows.

8) E.A. Guggenheim, "Thermodynamics," North-Holland Publishing Company, Amsterdam, 1977, Chapters 1 and 4.

Table I. The Values of Partition Coefficients

Liquid crystal substance	Solute	Transition[a]	$\lim_{x\to 0} (r)_{E=0}$
Cholesteryl myristate	*n*-Heptane	Sm-Ch	0.95
		Ch-Is	0.95
	n-Octane	Sm-Ch	0.84
		Ch-Is	0.89
	n-Nonane	Sm-Ch	0.87
		Ch-Is	0.82
Cholesteryl palmitate	*n*-Heptane	Sm-Ch	0.89
		Ch-Is	0.86
	n-Octane	Sm-Ch	0.87
		Ch-Is	0.80
	n-Nonane	Sm-Ch	0.76
		Ch-Is	0.72

a) Sm-Ch: Smectic-cholesteric transition, Ch-Is: cholesteric-isotropic transition.

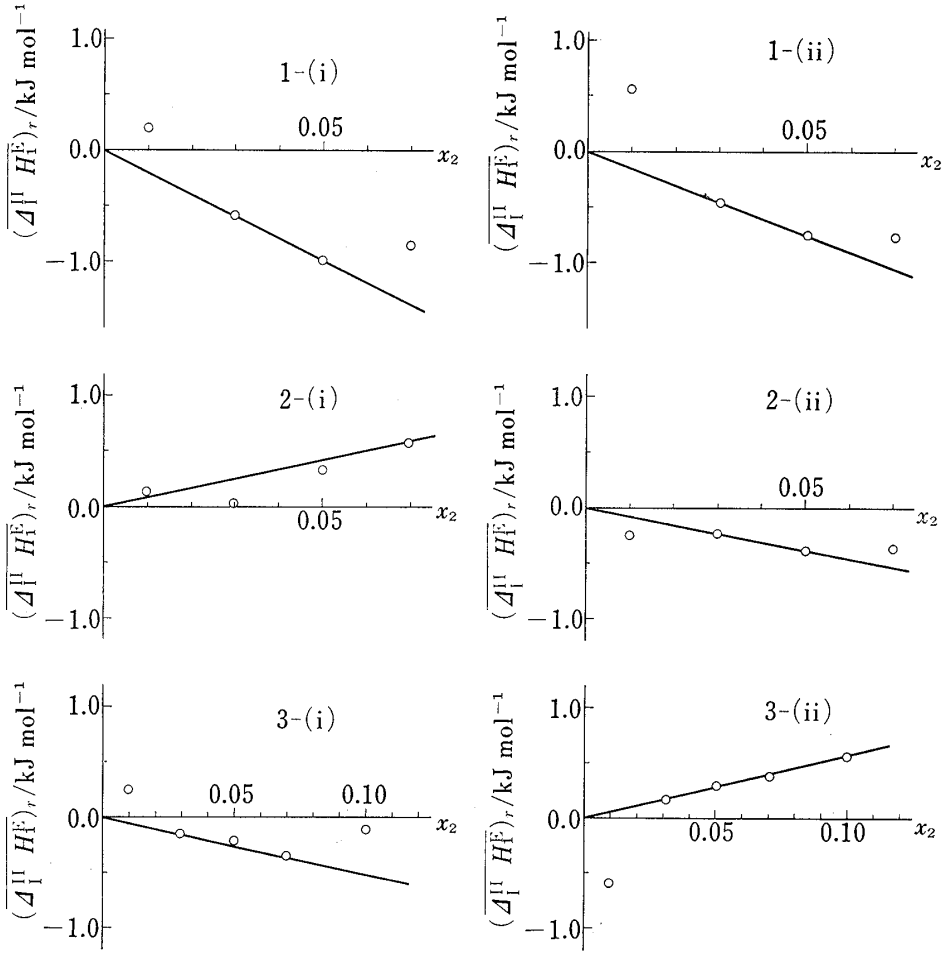

Fig. 9. $\overline{(\Delta_I{}^{II}\ H_1{}^E)_r}$ *vs.* x_2 in ChM-Alkane Systems

$\overline{(\Delta_I{}^{II}\ H_1{}^E)_r}$ means the molar transition excess enthalpy of the liquid crystal substance calculated by using the extrapolated value, $\lim_{x\to 0} (r)_{E=0}$, as the partition coefficient, r. See the text for details.

1: *n*-heptane, 2: n-octane, 3: *n*-nonane.

(i): smectic-cholesteric transition, (ii): cholesteric-isotropic transition.

$$x_2^{II} \approx \frac{2x_2}{1+r} \tag{11}$$

With Eq. (7), we finally have

$$\Delta T_{tr} \approx \frac{RT'_{tr}T^0_{tr}}{\Delta_I^{II}H_1^{\ominus} + \overline{\Delta_I^{II}H_1^E}} \cdot \frac{2(1-r)}{1+r} \cdot x_2(1+x_2), \tag{12}$$

where and hereafter ΔT_{tr} denotes $T'_{tr}-T^0_{tr}$ in place of $T_{tr}-T^0_{tr}$ in Eq. (7).

Taking into consideration the thermodynamic requirement that $\overline{\Delta_I^{II}H_1^E}$ approaches zero as the content of solute decreases, we assumed a zero value of $\overline{\Delta_I^{II}H_1^E}$ initially and calculated the values of r at various values of x_2 by substitution of T^0_{tr}, T'_{tr} and $\overline{\Delta_I^{II}H_1^E}$ into Eq. (12). Plots of these r values, denoted by $(r)_{E=0}$, *vs.* x_2 were linear, having very slight slopes. The extrapolated values of $(r)_{E=0}$ at $x=0$, which will be denoted by $\lim_{x\to 0}(r)_{E=0}$, are shown in Table I, although most values of $\lim_{x\to 0}(r)_{E=0}$ were not very different from $(r)_{E=0}$ at finite x_2.

In the solid-smectic transition of ChM-alkane systems and in the solid-cholesteric transition of ChP-alkane systems, the value of r or $\lim_{x\to 0}(r)_{E=0}$ was nearly equal to zero, implying equilibrium between pure ChM or ChP solid and liquid crystal mixture. Excluding these transitions, we shall proceed as follows. For the other transitions, we used the above-mentioned $\lim_{x\to 0}(r)_{E=0}$ at finite x_2 and calculated the values of $\overline{\Delta_I^{II}H_1^E}$, which will be denoted by $(\overline{\Delta_I^{II}H_1^E})_r$ and are shown in Figs. 9 and 10. Simulated curves of T'_{tr} *vs.* x_2 could be obtained by the substitution of $(\overline{\Delta_I^{II}H_1^E})_r$ at various values of x_2 and $\lim_{x\to 0}(r)_{E=0}$ into Eq. (12), as shown in Figs. 11 and 12. The simulation, even at this step, was good. The value of

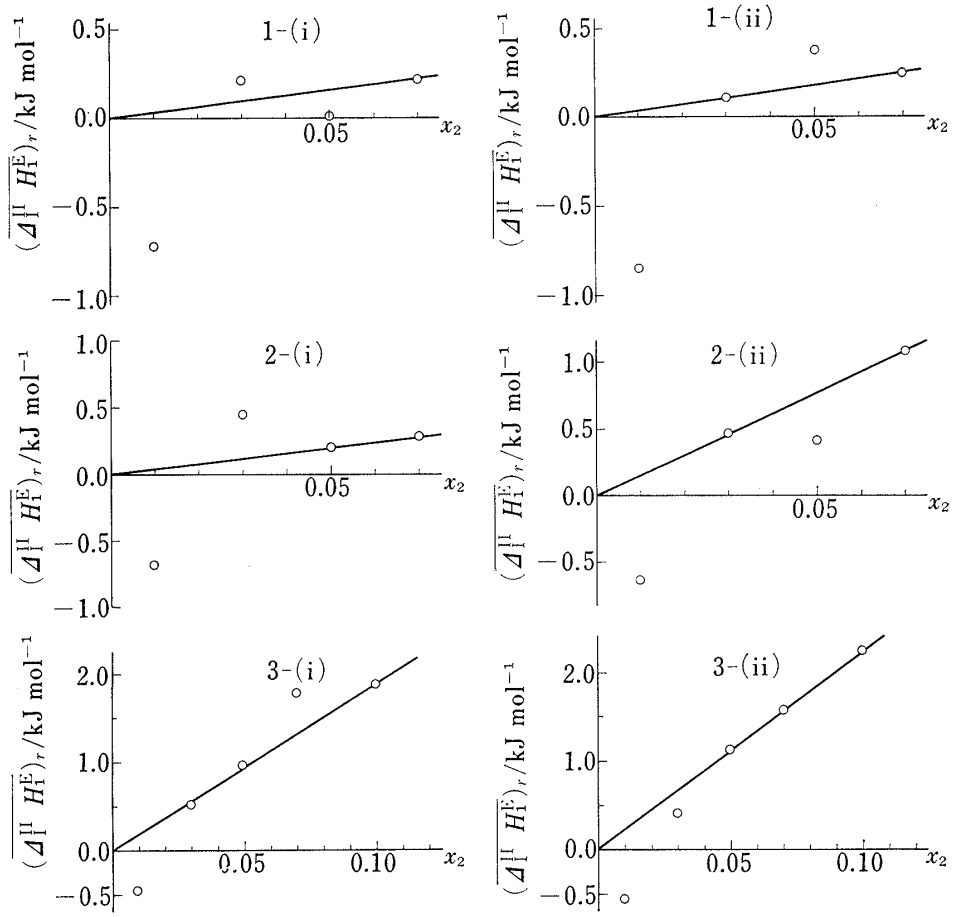

Fig. 10. $(\overline{\Delta_I^{II}H_1^E})_r$ *vs.* x_2 in ChP-Alkane Systems

Symbols are the same as in Fig. 9.

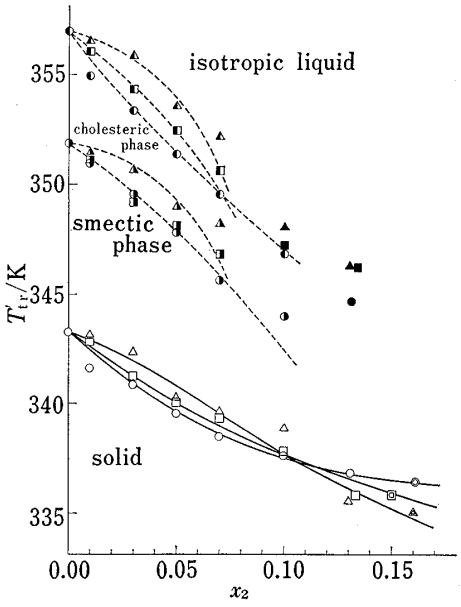

Fig. 11. Relation between T'_{tr} and x_2 in ChM-Alkane Systems

T'_{tr} is the characteristic temperature corresponding to point m in Fig. 1. Experimentally obtained values are shown by symbols similar to those in Fig. 4. Eq. (12) and (13) give the dotted and solid lines, respectively, with appropriate r and $\overline{(\Delta_I{}^{II} H_1{}^E)_r}$ values.

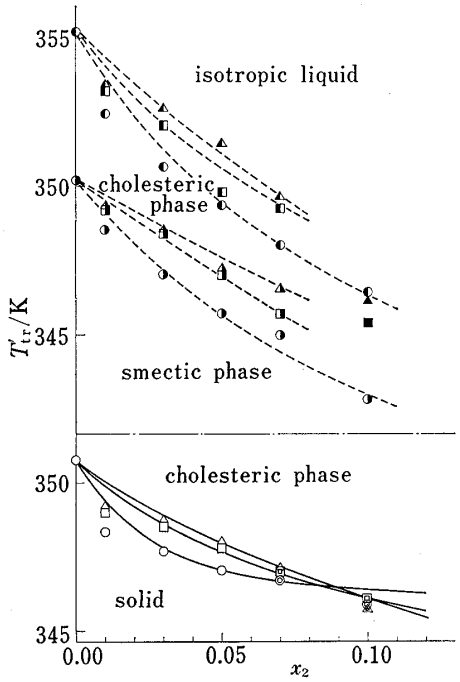

Fig. 12. Relation between T'_{tr} and x_2 in ChP-Alkane Systems

T'_{tr} is the characteristic temperature corresponding to point m in Fig. 1. Experimentally obtained values are shown by symbols similar to those in Fig. 4. Eq. (12) and (13) give the dotted and solid lines, respectively, with appropriate r and $\overline{(\Delta_I{}^{II} H_1{}^E)_r}$ values.

$\overline{\Delta_I{}^{II} H_1{}^E}$ which gives the best simulation will probably have an intermediate value between zero and the approximate $\overline{(\Delta_I{}^{II} H_1{}^E)_r}$.

In the solid-smectic transition of ChM-alkane systems and in the solid-cholesteric transition of ChP-alkane systems, we obtain Eq. (13) by the substitution of $r=0$ in Eq. (12), for the reasons mentioned already.

$$\Delta T_{tr} \approx \frac{R T'_{tr} T^0_{tr}}{\Delta_I{}^{II} H_1{}^{\ominus} + H_1{}^{II,E}} \cdot 2x_2(1+x_2) \qquad (13)$$

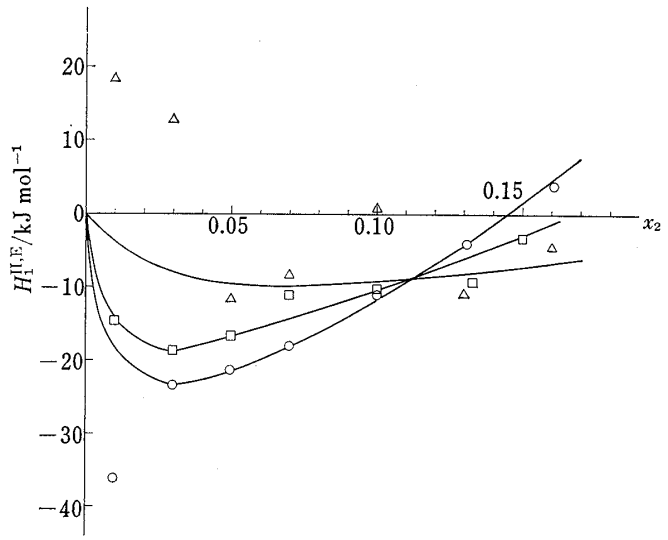

Fig. 13a. $H_1{}^{II,E}$ *vs.* x_2 Plot in ChM-Alkane Systems

$H_1{}^{II,E}$ is the molar excess enthalpy of ChM in the smectic phase.
△: *n*-heptane, □ :*n*-octane, ○ :*n*-nonane.

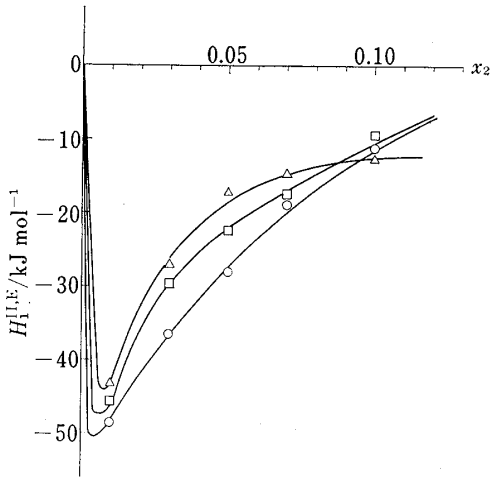

Fig. 13b. $H_1{}^{II,E}$ *vs.* x_2 Plot in Chp-Alkane Systems

$H_1{}^{II,E}$ is the molar excess enthalpy of ChP in the cholesteric phase.
△: *n*-heptane, □: *n*-octane, ○: *n*-nonane.

Figs. 13 a and b show the values of $H_1^{II,E}$ calculated by substitution of experimental ΔT_{tr} values at various x_2 in Eq. (13). The interpolated values of $H_1^{II,E}$, which fit the smoothed $H_1^{II,E}$ *vs.* x_2 curves, give the simulated T'_{tr} *vs.* x_2 curves in Figs. 11 and 12.

In the previous papers,[5,6] we determined the specific retention volume of component 2 in 1, V_g, by gas-liquid chromatography. The partition coefficient of component 2, k, between the gaseous phase and liquid phase (component 1) can be calculated as follows.

$$k = \frac{V_g T \rho_1}{273.15\mathrm{K}}, \tag{14}$$

where ρ_1 denotes the density of pure component 1. Considering a hypothetical three-phase equilibrium among gaseous phase and liquid phases I and II, we have

$$k^I = \frac{x_2^I N^I}{x_2^G N^G}, \quad k^{II} = \frac{x_2^{II} N^{II}}{x_2^G N^G}, \tag{15}$$

where k^I or k^{II} represents the partition coefficient of component 2 between the gaseous phase and phase I or II, respectively, and the superscript G shows the quantity in the gaseous phase, which is present in an infinitely small amount. Meanwhile, the partition coefficient K of component 2 between phases I and II is given by Eq. (16).

$$K = \frac{\gamma_2^I x_2^I}{\gamma_2^{II} x_2^{II}}, \tag{16}$$

where γ_2^I and γ_2^{II} represent the activity coefficients of component 2 in phases I and II. By the combination of Eq. (14), (15) and (16), we have

$$K = \frac{\gamma_2^I}{\gamma_2^{II}} \cdot \frac{V_g^I T^I \rho_1^I}{V_g^{II} T^{II} \rho_1^{II}} \cdot \frac{N^{II}}{N^I}. \tag{17}$$

At the transition temperature, where $T^I = T^{II}$ and $N^I \approx N^{II}$, we have

$$r \approx \frac{V_g^I}{V_g^{II}} \cdot \frac{\rho_1^I}{\rho_1^{II}}, \tag{18}$$

where r denotes x_2^I/x_2^{II} as already defined. As ρ_1^I/ρ_1^{II} was reported to be nearly equal to unity within ± 0.001,[9] we have

$$r \approx \frac{V_g^I}{V_g^{II}}. \tag{19}$$

The value of r, obtained from gas-liquid chromatographic data,[5,6] was unity within experimental error, while the value of $\lim_{x \to 0} (r)_{E=0}$, as shown in Table I, fell below unity. However, the difference between these values can be considered to be small, since not r but the logarithm of r contributes to the thermodynamic state of the system.

Conclusions

1. The polymorphism of ChM and ChP, *i.e.*, solid, smectic, cholesteric and isotropic phases, was maintained in spite of the addition of *ca.* 0.06 molar ratio of normal alkanes. However, the presence of alkanes decreases the distinctions in energy and entropy between coexisting phases, resulting in the disappearance of the cholesteric and smectic phases, successively.

2. The addition of alkanes markedly depresses the transition temperature; this could be described quantitatively by thermodynamic analysis, taking into consideration the partition of alkanes between coexisting phases. The partition coefficients agreed reasonably well with those previously obtained by gas-liquid chromatography.

Acknowledgement The authors thank Prof. K. Ikeda of our faculty and his staff for permission to use the DSC apparatus.

9) D. Demus, H.-G. Hahn, and F. Kuschel, *Mol. Cryst. Liq. Cryst.*, **44**, 61 (1978).